



MONTCLAIR STATE
UNIVERSITY

Montclair State University
**Montclair State University Digital
Commons**

Theses, Dissertations and Culminating Projects

5-2022

Modeling the Dynamics of Excitable Cells

Asja Alić

Follow this and additional works at: <https://digitalcommons.montclair.edu/etd>



Part of the [Applied Mathematics Commons](#), and the [Statistics and Probability Commons](#)

Abstract

We consider an electrical parallel conductance membrane model which is an extension of the classical Hodgkin-Huxley neuronal model of excitability. This extended model describes the formation of the resting membrane potential and conductance, and the formation of action potentials in nodose A-type excitable cells. The model consists of a set of nonlinear ordinary differential equations which are numerically solved using the Python programming language. The results show that the model is capable of accurately describing experimental results including resting membrane potential and conductance, duration and form of action potentials, amplitude of the spike, oscillations, and activity-dependent changes in $[Ca^{2+}]$ in the pericellular space and cytoplasm. This enables one to model the excitability of A-type nodose sensory neurons as well as to study the effects of ion channel modulators and their combinations under different environmental conditions such as variable extracellular Na^+ , K^+ , and Ca^{2+} concentrations and pericellular volume. The effects of tetrodotoxin which is found in pufferfish, 4-Aminopyridine chemical compound, and iberiotoxin which is found in the Indian Red Scorpion, were studied.

MONTCLAIR STATE UNIVERSITY

Modeling the Dynamics of Excitable Cells

by

Asja Alić

A Master's Thesis Submitted to the Faculty of

Montclair State University

In Partial Fulfillment of the Requirements

For the Degree of

Master of Science

May 2022

College of Science and Mathematics

Department of Applied
Mathematics and Statistics

Thesis Committee:

[REDACTED]

Dr. Eric Forgoston
Thesis Sponsor

[REDACTED]

Dr. Vladislav Snitsarev
Committee Member

[REDACTED]

Dr. Elena Petroff
Committee Member

MODELING THE DYNAMICS OF EXCITABLE CELLS

A THESIS

Submitted in partial fulfillment of the requirements

For the degree of Master of Science

by

ASJA ALIĆ

Montclair State University

Montclair, NJ

May 2022

Acknowledgements

I would like to thank my advisor, Dr. Eric Forgoston, for his help and guidance with this thesis. His support and knowledge have been invaluable throughout this process and I am very grateful.

I would also like to thank my committee members, Dr. Vladislav Snitsarev for his contributions, and Dr. Elena Petroff for her input, and to both for their support of my work.

I would also like to thank my family and friends for encouraging and motivating me in this process.

Contents

1	Introduction and Background	5
1.1	Hodgkin-Huxley Model	8
2	Extended Hodgkin-Huxley-Type Model	11
2.1	Model Development	12
3	Results	16
3.1	A-type Model	16
3.2	The Effect of Toxin	19
3.2.1	Tetrodotoxin	19
3.2.2	4-Aminopyridine	20
3.2.3	Iberiotoxin	23
4	Summary and Remarks	24

List of Figures

1	Electrical equivalent circuit for a short segment of a squid's giant axon. In the Hodgkin-Huxley model, the current is carried through the membrane by either charging the membrane capacitance C_m , or through movement of specific types of ions across the membrane, I_{Na} , I_K , and I_L [1].	7
2	Voltage, V_m (upper panel) and external current I_{ext} (lower panel) as a function of time found by solving Equations (8)-(11) using the parameter values in Table 1. The smaller stimulus generates a single action potential while the larger stimulus generates a train of action potentials.	11
3	Parallel conductance membrane model of a rat nodose neuron. (A) Equivalent circuit, where capacitance C_m is shunted by time- and voltage-dependent sodium, calcium, and potassium currents, a calcium ion activated potassium current, a transient outward current, a delay current, a leakage current, and electrogenic transporter-mediated currents. (B) Fluid compartment model which consists of three fluid compartments containing sodium, potassium, and calcium ions in different concentrations. The compartments include an intracellular space, an annular space, and an extracellular space [2].	14
4	Voltage, V_m , response to a stimulus injection of 0.04 nA, with all parameters at default values. A train of action potentials can be observed (top left) due to a stimulus current (top right). A whole cell current density phase portrait (bottom), shows a closed path in the phase plane as the neuron progresses through the action potentials (top left). . . .	20
5	Voltage, V_m response to a current stimulus injection of (a) 0.01nA, and (b) 0.02nA. In both instances the stimulus injection is too weak to generate any action potentials. (c) Voltage, V_m response to a stimulus injection of 0.03nA, which causes a single action potential. (d) Voltage, V_m response to a current stimulus injection of 0.04nA, and (e) 0.05nA. In both (d) and (e), a train of action potentials is observed, with the train in (e) showing a stronger intensity. Lastly, a case of overstimulation is shown in (f), due to a stimulus injection of 0.5nA. Too much stimulus caused the depression of this neuron.	21

List of Tables

1	Parameter values for the standard Hodgkin-Huxley model [1].	10
2	Inward Calcium Currents. Two calcium ion currents have been identified in rat nodose sensory neurons: one exhibiting transient dynamics $I_{Ca,t}$; and one exhibiting long-lasting dynamics $I_{Ca,n}$ [2].	15

3	Inward Sodium Currents. Two sodium ion currents have been identified in rat nodose neurons: one large TTX-sensitive current exhibiting fast kinetics I_{Na_f} ; and one smaller TTX-insensitive current with slower kinetics I_{Na_s} [2].	16
4	Outward Potassium Currents. Four potassium ion currents have been identified in rat nodose neurons: a delayed rectifier current I_K ; two independent potassium ion currents, one exhibiting rapid kinetics I_A , and another which rapidly activates, but inactivates with slow voltage-independent time constant I_D ; and one calcium activated potassium current $I_{K,Ca}$ [2].	17
5	Background, voltage, and concentration-dependent currents. Most excitable cells employ ion exchange mechanisms and ATP dependent pumps to maintain intracellular homeostasis. Active transport of sodium, potassium, and calcium ions is credited to the three mechanisms shown in this table: sodium-calcium exchanger current I_{NaCa} ; calcium pump current I_{CaP} ; and sodium-potassium pump current I_{NaK} . The model also includes a background current I_B [2].	18
6	A-type model parameters and conductances for each ionic channel [2].	19
7	Tetrodotoxin (TTX) is a powerful neurotoxin found in pufferfish (top right), from which it derives its name. When fast sodium conductance, g_{Na_f} , is at its default value of $2.05\mu S$, and a stimulus of $0.04nA$ is applied, a normal and uninterrupted train of action potentials is observed (middle). When TTX is present in the system, the sodium channel is blocked so that $g_{Na_f} = 0.0\mu S$, and the action potentials are no longer generated (bottom).	22
8	4-Aminopyridine (4-AP) is a simple organic chemical compound (top), and is toxic to humans. When potassium conductance is $g_K = 0.0055\mu S$ and a stimulus injection of $0.02nA$ is applied, no action potential is observed (middle). At toxic doses, 4-AP blocks potassium ion channels, and $g_K = 0.0\mu S$, which results in hyperactivity (bottom).	23
9	Iberitoxin (IbTX) is an ion channel toxin refined from the Indian Red Scorpion (top). IbTX blocks calcium-activated potassium channels. In the absence of IbTX, with $g_{KCa} = 0.0065\mu S$, and with a stimulus injection of $0.04nA$, a healthy, uninterrupted train of action potentials can be observed (middle). In the presence of IbTX, $g_{KCa} = 0.0\mu S$, the number of action potentials is increased, and they become progressively depressed (bottom).	24

1 Introduction and Background

An action potential is a brief change in voltage across a cell membrane and occurs when the membrane potential of a specific cell rapidly rises and falls due to the flow of ions through the membrane channels [1,3]. Action potentials occurs in excitable cells, including muscle cells, nerve cells, and endocrine cells, to name a few. Cells maintain a negatively charged inside environment in comparison to its outside environment. This difference in charge is called a membrane potential. Membrane potential is the difference in electric potential between interior and exterior of the cell, and it varies based on the type of cell. Here, we consider neurons or nerve cells, whose resting membrane potential is typically between -55mV and -70mV [3]. The specific value of the resting potential depends on the types of ion channels that are open and the concentrations of different ions in the intracellular and extracellular fluids during the resting state [3].

During the resting state, all voltage-dependent ion channels are closed. Once the stimulus current is applied, a rapid change in voltage occurs and an action potential is generated. It is important to note that a sufficient current must be applied to trigger membrane depolarization. Depolarization is the phase of action potential generation during which a cell undergoes a change in electric charge, resulting in less negative charge inside the cell compared to the outside. This shift occurs during an action potential, when depolarization is significant enough to momentarily reverse polarity in the cell [4]. During the depolarization stage, voltage-gated sodium channels open due to an electrical stimulus, and as the sodium ions rush back into the cell, their positive charge changes the potential inside the cell [3].

Once the cell has been depolarized, sodium ion channels begin to close. Now, the positive charge inside the cell causes voltage-gated potassium channels to open, causing the efflux of potassium ions out of the cell. The membrane potential then becomes more negative, and starts approaching its resting potential [3]. This stage is referred to as repolarization. Typically, repolarization will go beyond the resting potential, resulting in hyperpolarization. The membrane potential becomes more negative, until all of the voltage-gated potassium channels close, and the cell returns to its resting potential. Once hyperpolarization occurs, the cell enters its refractory period. During the refractory period, which follows every action potential, a nerve cell is unable to generate an action potential [3].

Alan Hodgkin and Andrew Huxley performed a series of experiments on the giant axon of the squid throughout the 1940s and early 1950s, which led them to develop a mathematical model that describes the electrical potential in a membrane of excitable cells. The giant axon of the squid has a much larger diameter when compared to most axons in the squid nervous system, as well as other nervous systems [5]. Thanks to this, Hodgkin and Huxley were able to perform experiments that were not possible on smaller axons that were used in most studies at the time. They were able to determine that the electrical signal is the basis of neuronal communication, as well as how the electrical signal is generated and propagated along the axon [1].

Their experimental work led them to develop a mathematical model which was used to find novel behavior that was not verifiable at the time but was later confirmed

and found to be true. Based on the series of electrophysiological experiments performed on the giant axon of the squid, they found three different types of ion currents: Na^+ , K^+ , and leak current. These currents were incorporated into the mathematical model which is comprised of a set of differential equations that describe the ionic basis of the action potential. It was published in 1952 and is now known as the Hodgkin-Huxley model. In 1963 they won the Nobel Prize in Physiology and Medicine after demonstrating how their model could accurately predict the key biophysical properties of the action potential. The Hodgkin-Huxley model is the basis of most neuronal models [6].

The Hodgkin-Huxley model is based on the equivalent circuit that models the electrical properties of a nerve membrane. In the equivalent circuit shown in Figure 1, we see that the current flow has two main components: i) charging the membrane capacitance and ii) the movement of specific types of ions across the membrane [7]. As mentioned, the membrane of the giant axon of the squid has three types of ion channels: Na^+ , K^+ , and leak channel. The leak channels have relatively low conductance and are mainly responsible for the resting membrane potential. The sodium (Na^+) and potassium (K^+) ion channels are the ones that generate the action potential and their conductances are both dependent on the voltage. It is important to note that one set of voltage-dependent channels is specifically permeable to Na^+ ions, while another set is specifically permeable to K^+ ions [1].

The behavior of the electrical circuit shown in Figure 1 can be characterized by

$$c_m \frac{dV_m}{dt} + I_{ion} = I_{ext}, \quad (1)$$

where c_m is the membrane capacitance, V_m is the membrane potential, I_{ion} is the net ionic current that is flowing across the membrane, and I_{ext} is an externally applied current. Note that I_{ion} consists of three components, namely inward sodium current I_{Na} , outward potassium current I_{K} , and leak current I_L , which is typically small, and establishes the resting membrane potential. It is also worth mentioning that this is a fundamental equation that relates the currents flowing across the membrane to the change in membrane potential.

Each of the individual ionic currents represent the macroscopic currents that are flowing through a large population of individual ion channels. The total ionic current is the sum of all individual currents from all channel types found in the cell membrane, and can be represented as

$$I_{ion} = \sum_k I_k = \sum_k G_k (V_m - E_k), \quad (2)$$

where E_k is the equilibrium potential (the potential at which the net ionic current is equal to zero), V_m is the membrane potential, and G_k is the conductance, which is the reciprocal of the resistance R_k so that $G_k = \frac{1}{R_k}$. One can see in Equation (2) that the current is proportional to the conductance multiplied by the difference between the membrane potential and the equilibrium potential. This idea may be expanded to include the three ionic current components found in the well-known Hodgkin-Huxley

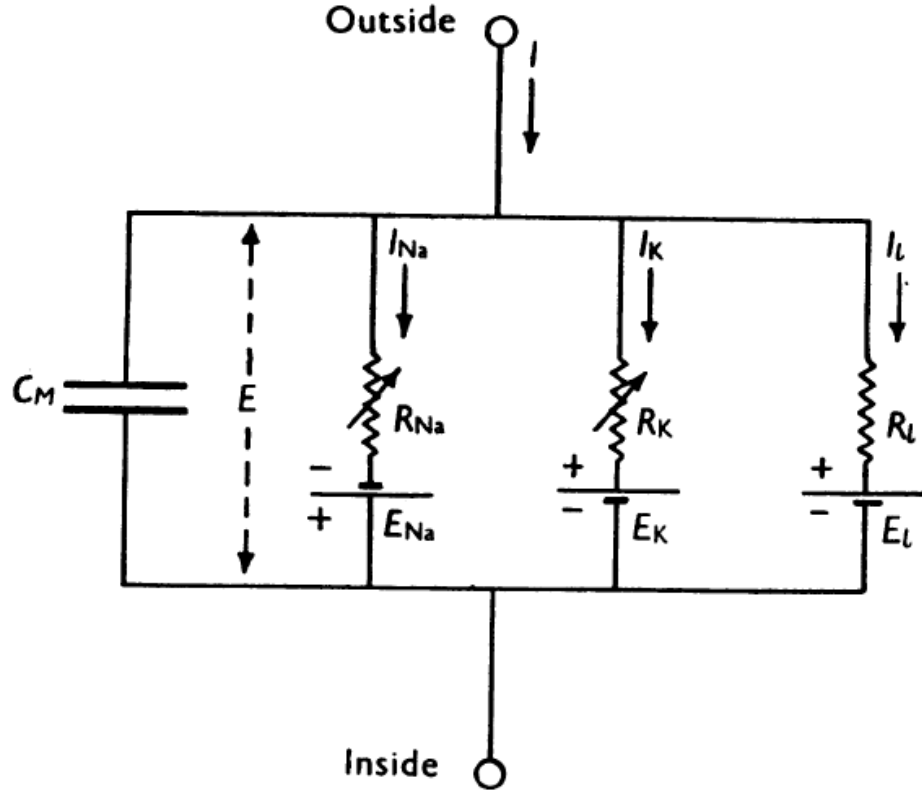


Figure 1: Electrical equivalent circuit for a short segment of a squid's giant axon. In the Hodgkin-Huxley model, the current is carried through the membrane by either charging the membrane capacitance C_m , or through movement of specific types of ions across the membrane [1].

model so that

$$I_{ion} = G_{Na}(V_m - E_{Na}) + G_K(V_m - E_K) + G_L(V_m - E_L). \quad (3)$$

Hodgkin and Huxley suggested that the sodium and potassium currents were voltage-dependent, while the leakage current was constant. At the time of their investigation, they did not know all the properties of individual membrane channels, but today we know that voltage dependence of sodium and potassium currents can be related to the biophysical properties of individual ion channels that contribute to these macroscopic conductances.

One can visualize that each ion channel has one or more gates that are arranged one after another. In order for the channel to be open and allow ions to flow through, each of the gates needs to be open at the same time. Otherwise the whole channel is closed. When the channel is open and ions are able to pass through, we say the gates are in a permissive state. On the other hand, when the channel is closed and ions are unable to pass through, we say the gates are in a non-permissive state [1]. The probability of the gate being in either a permissive or non-permissive state depends on the voltage across the membrane. These channel gates fall into two classes: i) activation gates, and ii) inactivation gates.

For activation gates, the probability of the gate being open increases with depolarization, whereas for inactivation gates, the probability of the gate being open decreases with depolarization. The probability of a gate being open at any time is known as the activation variable for that gate. Each Na channel contains a set of three rapidly responding activation gates known as the m -gates, and a single, slower responding, inactivation gate, known as the h -gate [1].

For the sodium channel, the h -gate is open at resting potential, while the m -gates are shut, so the channel itself is shut. If the membrane is then depolarized, the m -gates rapidly open, and for a while the channel itself is open or activated. Then the h -gate shuts, and therefore the channel shuts, even though the membrane is still depolarized. The channel is now in the inactivated state. If the membrane is now repolarized, the m -gates rapidly shut. If the membrane is again depolarized, the m -gates open, but the h -gate remains shut, and so the channel itself does not reopen. Finally, if the membrane is repolarized the m -gates shut, and if the membrane is held repolarized for some time, the h -gate eventually reopens (de-inactivation). The channel is now back in its original condition; shut, but ready to open in response to depolarization [1].

The potassium channel is slightly simpler, as it contains only a single gate that consists of four individual activation n -gates, which respond more slowly than the gates of the sodium channel. Therefore, if the membrane is depolarized the n -gates open slowly and the potassium channel opens. The channel will remain open as long as the membrane remains depolarized [1]. Once the membrane is repolarized the n -gates slowly shut.

1.1 Hodgkin-Huxley Model

When an individual channel opens, it contributes a small amount to the total conductance, and contributes none when closed. Therefore, the macroscopic conductance for a large population of channels is proportional to the number of channels in the open state, which is proportional to the probability that the associated gates are in a permissive state [5]. The macroscopic conductance, G_k , is proportional to the product of the individual gate probabilities p_i so that

$$G_k = \bar{g}_k \prod p_i, \quad (4)$$

where \bar{g}_k is a normalization constant that determines the maximum possible conductance when all the channels are open.

Sodium conductance is modeled with three m -gates and one h -gate as

$$G_{\text{Na}} = \bar{g}_{\text{Na}} m^3 h, \quad (5)$$

while potassium conductance is modeled with four identical n -gates as

$$G_{\text{K}} = \bar{g}_{\text{K}} n^4. \quad (6)$$

Equation (3), which describes the ionic currents in the Hodgkin-Huxley model can thus be written as

$$I_{\text{ion}} = \bar{g}_{\text{Na}} m^3 h (V_m - E_{\text{Na}}) + \bar{g}_{\text{K}} n^4 (V_m - E_{\text{K}}) + \bar{g}_L (V_m - E_L). \quad (7)$$

Substitution of Equation (7) into Equation (1) shows that

$$\frac{dV_m}{dt} = \frac{1}{c_m} [I_{ext} - (\bar{g}_{Na} m^3 h (V_m - E_{Na}) + \bar{g}_K n^4 (V_m - E_K) + \bar{g}_L (V_m - E_L))]. \quad (8)$$

Furthermore, the values of m , h , and n can be determined by integrating the following equations

$$\frac{dm}{dt} = \alpha_m(V)(1 - m) - \beta_m(V)m, \quad (9)$$

$$\frac{dh}{dt} = \alpha_h(V)(1 - h) - \beta_h(V)h, \quad (10)$$

$$\frac{dn}{dt} = \alpha_n(V)(1 - n) - \beta_n(V)n, \quad (11)$$

where α_i and β_i are voltage-dependent rate constants describing respectively the non-permissive to permissive transition rates, and the permissive to non-permissive transition rates [1].

To solve the system of equations given by Equations (8)-(11), one needs initial conditions and values for the various parameters. We obtain these values by solving for resting values of m , h , and n . When $V = 0$, m , h , and n have resting values given by

$$m_0 = \frac{\alpha_{m0}}{\alpha_{m0} + \beta_{m0}}, \quad (12)$$

$$h_0 = \frac{\alpha_{h0}}{\alpha_{h0} + \beta_{h0}}, \quad (13)$$

$$n_0 = \frac{\alpha_{n0}}{\alpha_{n0} + \beta_{n0}}. \quad (14)$$

If V is suddenly changed, α_i and β_i take on values according to the new voltage. The solution of Equations (9)-(11) that satisfies the boundary conditions $m = m_0$, $h = h_0$, and $n = n_0$, when $t = 0$ is [1]

$$m = m_\infty - (m_\infty - m_0) \exp(-t/\tau_m), \quad (15)$$

$$h = h_\infty - (h_\infty - h_0) \exp(-t/\tau_h), \quad (16)$$

$$n = n_\infty - (n_\infty - n_0) \exp(-t/\tau_n), \quad (17)$$

where

$$m_\infty = \alpha_m / (\alpha_m + \beta_m), \quad (18)$$

$$\tau_m = 1 / (\alpha_m + \beta_m), \quad (19)$$

$$h_\infty = \alpha_h / (\alpha_h + \beta_h), \quad (20)$$

$$\tau_h = 1 / (\alpha_h + \beta_h), \quad (21)$$

$$n_\infty = \alpha_n / (\alpha_n + \beta_n), \quad (22)$$

$$\tau_n = 1 / (\alpha_n + \beta_n). \quad (23)$$

We further consider the voltage-dependent rate parameters that were obtained by Hodgkin and Huxley [1]. The rate constants for K activation are given as

$$\alpha_n = -\frac{0.01(V + 10)}{e^{\frac{V+10}{10}} - 1}, \quad (24)$$

$$\beta_n = 0.125e^{\frac{V}{80}}. \quad (25)$$

Similarly, the voltage dependence of the m and h gates of the sodium channel are given as

$$\alpha_m = \frac{0.1(V + 25)}{e^{\frac{V+25}{10}} - 1}, \quad (26)$$

$$\beta_m = 4e^{\frac{V}{18}}, \quad (27)$$

for Na activation, and as

$$\alpha_h = 0.07e^{\frac{V}{20}}, \quad (28)$$

$$\beta_h = \frac{1}{e^{\frac{V+30}{0.10}} + 1}, \quad (29)$$

for Na inactivation.

Figure 2 shows the result of solving the Hodgkin-Huxley system given by Equations (8)-(11) using the parameter values of Table 2. The results provide good agreement with Hodgkin and Huxley's experimental data [1].

Constants	Description
$c_m = 1.0 \frac{\mu F}{cm^2}$	Membrane capacitance
$\bar{g}_{Na} = 120 \frac{mS}{cm^2}$	Sodium maximum conductance
$\bar{g}_K = 36 \frac{mS}{cm^2}$	Potassium maximum conductance
$\bar{g}_L = 0.3 \frac{mS}{cm^2}$	Leak maximum conductance
$E_{Na} = 50.0mV$	Sodium reversal potential
$E_K = -77.0mV$	Potassium reversal potential
$E_{Na} = -54.387mV$	Leak reversal potential

Table 1: Parameter values for the standard Hodgkin-Huxley model [1].

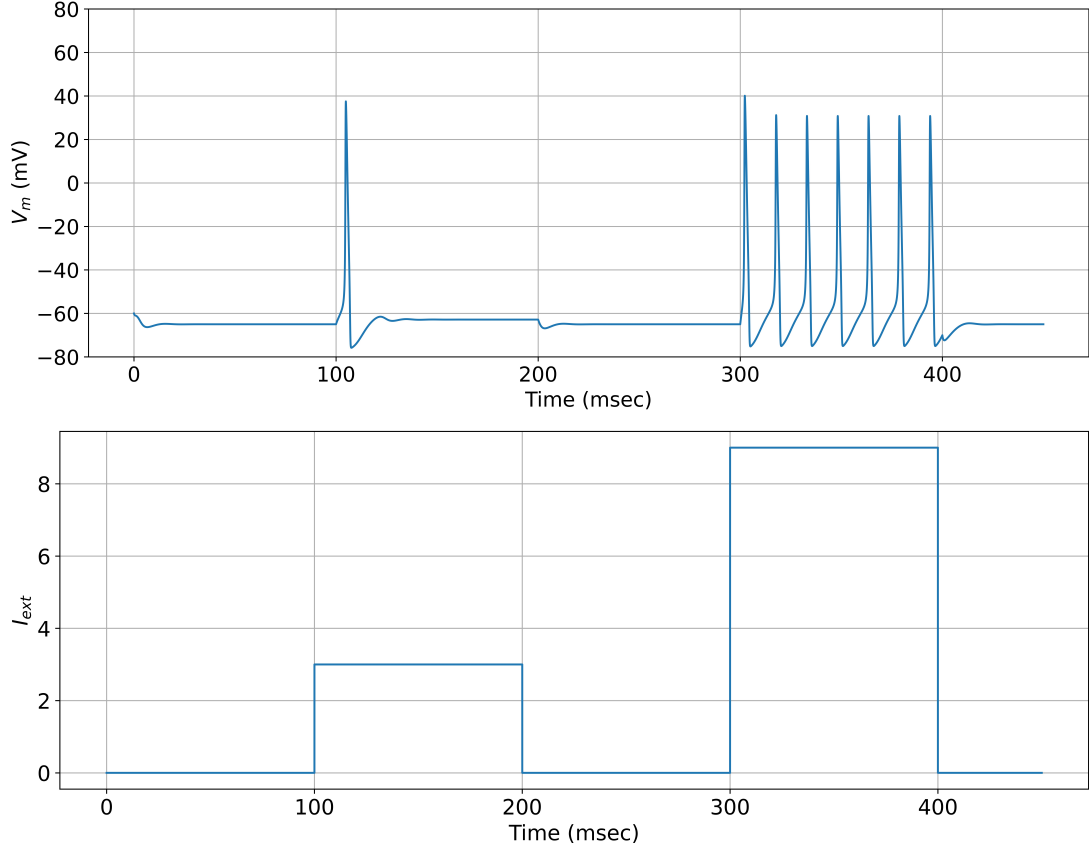


Figure 2: Voltage, V_m (upper panel) and external current I_{ext} (lower panel) as a function of time found by solving Equations (8)-(11) using the parameter values in Table 1. The smaller stimulus generates a single action potential while the larger stimulus generates a train of action potentials.

2 Extended Hodgkin-Huxley-Type Model

In Section 1, we presented the classical Hodgkin-Huxley model which is capable of accurately describing experimental results, including the duration and form of action potentials, amplitude of the spike, oscillations, and sodium and potassium ionic changes. We now consider an expanded version of this model which can accurately reproduce the electrical behavior of both A-type and C-type nodose sensory neurons, as well as the effects of known ion channel blockers [2].

This model consists of an expanded Hodgkin-Huxley-type membrane model coupled with a fluid compartment model that describes perinuclear and intracellular Ca^{2+} ion concentration dynamics. The model can be used to understand the electrical behavior of A-type and C-type nodose neurons when exposed to different stimulus environments. The model accurately describes the whole cell voltage-clamp recordings of all major ion channels, as well as the current-clamp recordings of action potential dynamics. Noting that one could easily study C-type neurons using the same model but with changes in parameter values, in this thesis we focus on A-type neurons.

2.1 Model Development

We use a general Hodgkin-Huxley-type description of whole-cell currents given as

$$I(t, V) = \bar{g}m^x(t, V)h^y(t, V)(V - E_i), \quad (30)$$

where \bar{g} represents the maximum whole-cell conductance, m and h are respectively the activation and inactivation gating variables, with corresponding integer exponents x and y , V is the membrane potential, and E_i is the Nernst reversal potential for the ion channel under consideration [2].

Channel gating variables are given as solutions to a first-order differential equation of the general form

$$\dot{z} = \frac{(z_\infty - z)}{\tau_z}, \quad (31)$$

where z represents the gating variable, z_∞ is the steady-state value of the gating variable, and τ_z is the voltage-dependent time constant associated with the gating variable z . For all currents, z_∞ is described using a standard Boltzmann function given by

$$z_\infty(V) = \frac{1.0}{1.0 + \exp\left(\frac{V_{1/2} - V}{S_{1/2}}\right)}, \quad (32)$$

where $V_{1/2}$ is the half-activation potential, and $S_{1/2}$ is related to the reciprocal of the slope of the activation curve measured at $V_{1/2}$. The time constants, τ_z for both activation and inactivation are described using a Gaussian function of the form

$$\tau_z = A \exp(-B^2(V - V_{peak})^2) + C, \quad (33)$$

where A corresponds to the peak amplitude, B scales the function's width, V_{peak} corresponds to the membrane potential at which τ_z is equal to A , and C is an offset parameter.

Using this general Hodgkin-Huxley-type description of the model, equations can be formulated for each ionic membrane current. The complete model consists of lumped membrane capacitance C_m shunted by voltage- and time-dependent ion channels, as well as pump, exchanger, and other background currents. This membrane model is coupled with a fluid compartment model, which describes the intracellular and perinuclear Ca^{2+} dynamics within the intracellular (Vol_i) and perinuclear (Vol_p) volumes.

As with the Hodgkin-Huxley model described in Section 1, we consider the equivalent membrane circuit that models the electrical properties of the neuron. Figure 3(A) shows an equivalent circuit of the neuron where membrane capacitance C_m is shunted by time- and voltage-dependent sodium, calcium, and potassium currents (I_{Na_f} , I_{Na_s} , $I_{\text{Ca},t}$, $I_{\text{Ca},n}$, I_K), a Ca^{2+} activated potassium current ($I_{K,\text{Ca}}$), a transient outward current (I_A), a delay current (I_D), a linear leakage current (I_B), and electrogenic transporter-mediated currents ($\text{Na}^+ - \text{Ca}^{2+}$ exchanger, $\text{Na}^+ - \text{K}^+$ pump, Ca^{2+} pump). Additionally, E_{Na} , E_K , E_{Ca} , and E_B are the equilibrium potentials for the sodium, potassium, calcium, and background ionic channels, respectively [2]. Figure 3(B) shows the lumped fluid compartment model. The model consists of three fluid

compartments containing Na^+ , K^+ , and Ca^{2+} in different concentrations. We consider three compartments, namely an intracellular fluid space, a $1.0\mu\text{m}$ annular fluid space, and a large extracellular volume where all ionic concentrations are assumed to be constant [2].

Network analysis of the circuit shown in Figure 3 allows one to develop the differential equation describing the time-dependent changes in membrane potential (V_m) as

$$\dot{V}_m = -\frac{\Sigma I_{ion} - I_{ext}}{C_m}, \quad (34)$$

where I_{ion} corresponds to individual currents shown in the circuit in Figure 3(A), and I_{ext} corresponds to either the total evoked current as measured under voltage-clamp conditions, or the total injected current used in current-clamp conditions. Using Equations (30)-(33), one can form Hodgkin-Huxley-style differential equations for $z = m_f, h_f, h_s, d_t, f_t, d_n, f_{n1}, f_{n2}, n, p, q, x, y$ and c . The complete set of equations and parameters is presented in Tables 2-5.

Experiments have identified two inward currents for both calcium and sodium in rat nodose neurons. With regards to the Ca^{2+} currents, one of them demonstrates transient dynamics ($I_{\text{Ca},t}$), activates at membrane potentials near -70mV , and exhibits rapid inactivation. On the other hand, the second demonstrates long-lasting dynamics ($I_{\text{Ca},n}$), activates rapidly near -30mV and exhibits both a fast and a slow component of inactivation, as well as significant component of incomplete inactivation [2]. Table 2 provides all of the model equations for these currents. With regards to the two Na^+ currents, one of them is a large TTX-sensitive current, exhibiting fast kinetics ($I_{\text{Na},f}$), while the other is a smaller TTX-insensitive current with slower kinetics ($I_{\text{Na},s}$). Table 3 provides all of the model equations for these four inward currents.

In addition, there are four outward potassium currents. They include a large outwardly rectifying K^+ current (I_K), which is slow to activate, and exhibits no significant inactivation, a calcium activated potassium current ($I_{\text{K,Ca}}$), which is slow to activate at membrane potentials below 0mV , but increases rapidly above 10mV , and two transient outward potassium currents. Of the latter two currents, one exhibits rapid kinetics (I_A), while the other (I_D) rapidly activates but inactivates with a slow voltage-independent time constant [2]. Table 4 provides all of the model equations for these four outward currents.

We next consider the pump, exchanger and background currents. Most excitable cells employ ion exchange mechanisms and ATP-dependent pumps to maintain intracellular homeostasis. Therefore, any detailed Hodgkin-Huxley-based neuronal model must reflect these mechanisms. In the model that we are considering, active transport of calcium, sodium, and potassium ions across the neural membrane is accredited to the following three mechanisms: a high capacity sodium-calcium exchanger ($I_{\text{Na,Ca}}$), electrogenic calcium pump (I_{CaP}), and an electrogenic activated potassium pump ($I_{\text{K,Ca}}$) [2]. Table 5 provides all of the model equations for these three currents.

Lastly, the governing equations for the fluid compartment model described previously must be developed. The temporal rate of change in occupancy of a non-

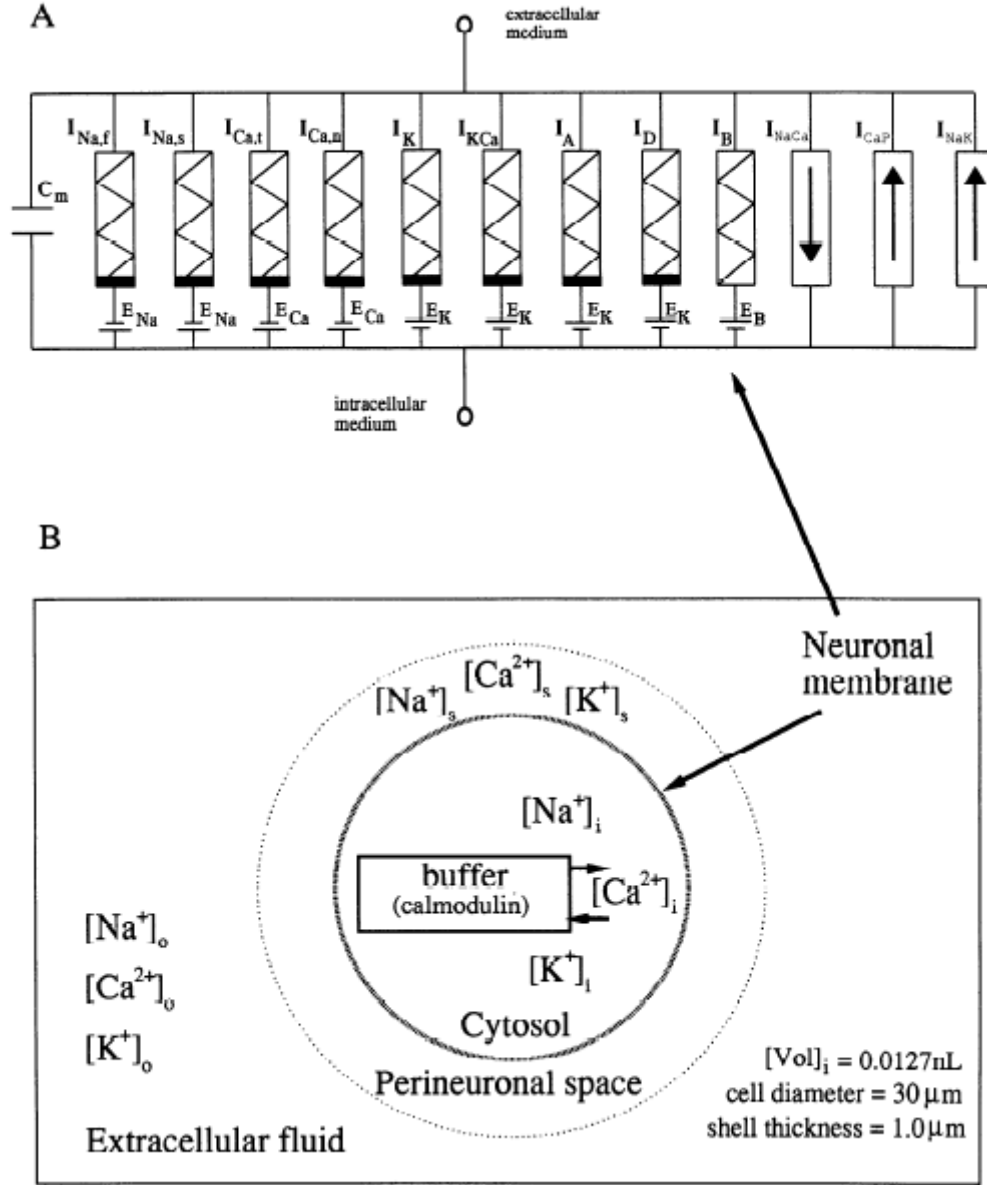


Figure 3: Parallel conductance membrane model of a rat nodose neuron. (A) Equivalent circuit, where capacitance C_m is shunted by time- and voltage-dependent sodium, calcium, and potassium currents, a calcium ion activated potassium current, a transient outward current, a delay current, a leakage current, and electrogenic transporter-mediated currents. (B) Fluid compartment model which consists of three fluid compartments containing sodium, potassium, and calcium ions in different concentrations. The compartments include an intracellular space, an annular space, and an extracellular space [2].

organelle-related intracellular buffer is described by

$$\dot{O}_c = k_U [Ca^{2+}]_i (1 - O_c) - k_R O_c, \quad (35)$$

$I_{Ca,t}$: Low Threshold, Transient Calcium Current		
$I_{Ca,t} = \bar{g}_{Ca,t} d_t f_t (V - E_{Ca})$		
$\dot{d}_t = \frac{d_{t\infty} - d_t}{\tau_{d_t}}$	$\dot{f}_t = \frac{f_{t\infty} - f_t}{\tau_{f_t}}$	$E_{Ca} = \frac{RT}{Z_{Ca}} \ln \frac{[Ca^{2+}]_s}{[Ca^{2+}]_i} - 78.7$
$\tau_{d_t} = 22.0 \exp(-(0.052)^2 (V + 68.0)^2) + 2.5$		
$\tau_{f_t} = 103.0 \exp(-(0.050)^2 (V + 58.0)^2) + 12.5$		
$d_{t\infty} = \frac{1.0}{1.0 + \exp\left(\frac{V+54.0}{-5.75}\right)}$		
$f_{t\infty} = \frac{1.0}{1.0 + \exp\left(\frac{V+68.0}{6.0}\right)}$		
$I_{Ca,n}$: High Threshold, Long-Lasting Calcium Current		
$I_{Ca,n} = \bar{g}_{Ca,n} d_n (0.55 f_{n1} + f_{n2} (V - E_{Ca}))$		
$\dot{d}_n = \frac{d_{n\infty} - d_n}{\tau_{d_n}}$	$\dot{f}_{n1} = \frac{f_{n1\infty} - f_{n1}}{\tau_{f_{n1}}}$	$\dot{f}_{n2} = \frac{f_{n2\infty} - f_{n2}}{\tau_{f_{n2}}}$
$\tau_{d_n} = 3.21 \exp((0.042)^2 (V + 31.0)^2) + 0.395$		
$\tau_{f_{n1}} = 33.5 \exp((0.0395)^2 (V + 30.0)^2) + 5.0$		
$\tau_{f_{n2}} = 225.0 \exp((0.0275)^2 (V + 40.0)^2) + 75.0$		
$d_{n\infty} = \frac{1.0}{1.0 + \exp\left(\frac{V+20.0}{-4.5}\right)}$		
$r_n = \frac{0.2}{1.0 + \exp\left(\frac{V+5.0}{-10}\right)}$		
$f_{n1\infty} = \frac{1.0}{1.0 + \exp\left(\frac{V+20.0}{25.0}\right)}$		
$f_{n2\infty} = r_n + \frac{1.0}{1.0 + \exp\left(\frac{V+5.0}{-10.0}\right)}$		

Table 2: Inward Calcium Currents. Two calcium ion currents have been identified in rat nodose sensory neurons: one exhibiting transient dynamics $I_{Ca,t}$; and one exhibiting long-lasting dynamics $I_{Ca,n}$ [2].

where O_c is the buffer occupancy, and k_U and k_R are the kinetic rate constants for Ca^{2+} uptake and release, respectively [2]. The rate of change of intracellular Ca^{2+} ion concentration is described by

$$[Ca^{2+}]_i = \frac{2I_{Na,Ca} - I_{Ca,n} - I_{Ca,t} - I_{B,Ca} - I_{CaP}}{Z_{Ca} Vol_i F} - n_b [B]_i \dot{O}_c, \quad (36)$$

where Z_{Ca} is the valence, F is Faraday's constant, and Vol_i is an effective cell volume [2]. A similar expression, formed to account for Ca^{2+} balance within the external perinuclear space (Vol_p), is given as

$$[Ca^{2+}]_s = \frac{[Ca^{2+}]_o - [Ca^{2+}]_s}{\tau_{Ca}} + \frac{-2I_{Na,Ca} + I_{Ca,n} + I_{Ca,t} + I_{B,Ca} + I_{CaP}}{Z_{Ca} Vol_s F}, \quad (37)$$

I_{Na_f} : Fast, TTX Sensitive Sodium Current	
$I_{\text{Na}_f} = \bar{g}_{\text{Na}_f} m_f^3 h_f (V - E_{\text{Na}})$	
$\dot{m}_f = \frac{m_{f\infty} - m_f}{\tau_{m_f}}$	$\dot{h}_f = \frac{h_{f\infty} - h_f}{\tau_{h_f}}$
$\tau_{m_f} = 1.15 \exp((0.06)^2 (V + 40.0)^2) + 0.21$	
$\tau_{h_f} = 18.0 \exp((0.043)^2 (V + 62.5)^2) + 1.35$	
$m_{f\infty} = \frac{1.0}{1.0 + \exp\left(\frac{V+31.6}{-6.98}\right)}$	$h_{f\infty} = \frac{1.0}{1.0 + \exp\left(\frac{V+66.0}{-5.97}\right)}$
I_{Na_s} : Slower, TTX Insensitive Sodium Current	
$I_{\text{Na}_s} = \bar{g}_{\text{Na}_s} m_s^3 h_s (V - E_{\text{Na}})$	
$\dot{m}_s = \frac{m_{s\infty} - m_s}{\tau_{m_s}}$	$\dot{h}_s = \frac{h_{s\infty} - h_s}{\tau_{h_s}}$
$\tau_{m_s} = 1.45 \exp((0.058)^2 (V + 14.5)^2) + 0.26$	
$\tau_{h_s} = 10.75 \exp((0.067)^2 (V + 13.5)^2) + 3.15$	
$m_{s\infty} = \frac{1.0}{1.0 + \exp\left(\frac{V+11.3}{-5.45}\right)}$	$h_{s\infty} = \frac{1.0}{1.0 + \exp\left(\frac{V+31.0}{5.2}\right)}$

Table 3: Inward Sodium Currents. Two sodium ion currents have been identified in rat nodose neurons: one large TTX-sensitive current exhibiting fast kinetics I_{Na_f} ; and one smaller TTX-insensitive current with slower kinetics I_{Na_s} [2].

where τ_{Ca} represents the relatively slow time constant for Ca^{2+} ion diffusion between the perinuclear volume and the bathing medium, and Vol_s is the annular shell thickness [2]. Table 6 provides parameter values needed for the fluid compartment equations along with the required model parameters and maximum whole-cell conductances for the A-type neuron model. The derivation of the governing equations for the extended Hodgkin-Huxley-type model can be found in Ref. [2].

3 Results

3.1 A-type Model

As discussed previously, the extended model consists of a Hodgkin-Huxley-type membrane model which is coupled to a fluid compartment model for the Ca^{2+} dynamics. The model accurately reproduces whole-cell voltage-clamp and current-clamp recordings of the major ion channel currents. Moreover, this model realistically emulates the electrical behavior of A-type nodose sensory neurons under a wide variety of current

I_K : Delayed Rectifier	
$I_K = \bar{g}_K n (V - E_K)$	$\dot{n} = \frac{n_\infty - n}{\tau_n}$
$\tau_n = \frac{1.0}{(\alpha_n + \beta_n)}$	$n_\infty = \frac{1.0}{1.0 + \exp\left(\frac{V+14.62}{-18.38}\right)}$
$\alpha_n = \frac{0.001265(V+14.273)}{1.0 - \exp\left(\frac{V+14.273}{-10.0}\right)}$	$\beta_n = 0.125 \exp\left(\frac{V+55.0}{-2.5}\right)$
I_A : Early Transient Outward Current	
$I_A = \bar{g}_A p^3 q (V - E_K)$	
$\dot{p} = \frac{p_\infty - p}{\tau_p}$	$\dot{q} = \frac{q_\infty - q}{\tau_q}$
$\tau_p = 5.0 \exp\left((0.22)^2 (V + 65.0)^2\right) + 2.5$	
$\tau_q = 100.0 \exp\left((0.035)^2 (V + 30.0)^2\right) + 10.5$	
$p_\infty = \frac{1.0}{1.0 + \exp\left(\frac{V+28.0}{-28}\right)}$	$q_\infty = \frac{1.0}{1.0 + \exp\left(\frac{V+58.0}{7.0}\right)}$
I_D : Slowly Inactivating Delay Current	
$I_D = \bar{g}_D x^3 y (V - E_K)$	
$\dot{x} = \frac{x_\infty - x}{\tau_x}$	$\dot{y} = \frac{y_\infty - y}{\tau_y}$
$\tau_x = 5.0 \exp\left((0.022)^2 (V + 65.0)^2\right) + 2.5$	$\tau_y = 7500.0$
$x_\infty = \frac{1.0}{1.0 + \exp\left(\frac{V+39.59}{-14.68}\right)}$	$y_\infty = \frac{1.0}{1.0 + \exp\left(\frac{V+48.0}{7.0}\right)}$
$I_{K,Ca}$: Calcium-Activated Potassium Current	
$I_{K,Ca} = \bar{g}_{K,Ca} c (V - E_K)$	$\dot{c} = \frac{c_\infty - c}{\tau_c}$
$\alpha_c = 750.0 [Ca^{2+}]_i \exp\left(\frac{V-10.0}{12.0}\right)$	$\beta_c = 0.05 \exp\left(\frac{V-10.0}{-60.0}\right)$
$\tau_c = \frac{4.5}{\alpha_c + \beta_c}$	$c_\infty = \frac{\alpha_c}{c + \beta_c}$

Table 4: Outward Potassium Currents. Four potassium ion currents have been identified in rat nodose neurons: a delayed rectifier current I_K ; two independent potassium ion currents, one exhibiting rapid kinetics I_A , and another which rapidly activates, but inactivates with slow voltage-independent time constant I_D ; and one calcium activated potassium current $I_{K,Ca}$ [2].

I_B : Background Current
$I_B = I_{B,Na} + I_{B,Ca} = \bar{g}_{B,Na}(V - E_{Na}) + \bar{g}_{B,Ca}(V - E_{Ca})$
$I_{Na,Ca}$: Sodium-Calcium Exchanger Current
$I_{NaCa} = I_{NaCa} \frac{DF_{in} - DF_{out}}{S}$
$S = 1.0 + D_{NaCa}([Ca^{2+}]_i[Na^+]_o + [Ca^{2+}]_s[Na^+]_i)$
$DF_{in} = [Na^+]_i^r [Ca^{2+}]_s \exp\left(\frac{(r-2)\gamma VF}{RT}\right)$
$DF_{out} = [Na^+]_o^r [Ca^{2+}]_i \exp\left(\frac{(r-2)(\gamma-1)VF}{RT}\right)$
I_{CaP} : Calcium Pump Current
$I_{CaP} = \bar{I}_{CaP} \left(\frac{[Ca^{2+}]_i}{[Ca^{2+}]_i + K_{M,CaP}}\right)$
I_{NaK} : Sodium-Potassium Pump Current
$I_{NaK} = \bar{I}_{NaK} \left(\frac{[Na^+]_i}{[Na^+]_i + K_{M,Na}}\right)^3 \left(\frac{[K^+]_o}{[K^+]_o + K_{M,K}}\right)^2 \left(\frac{V+150}{V+200}\right)$

Table 5: Background, voltage, and concentration-dependent currents. Most excitable cells employ ion exchange mechanisms and ATP dependent pumps to maintain intracellular homeostasis. Active transport of sodium, potassium, and calcium ions is credited to the three mechanisms shown in this table: sodium-calcium exchanger current I_{NaCa} ; calcium pump current I_{CaP} ; and sodium-potassium pump current I_{NaK} . The model also includes a background current I_B [2].

stimulus injections and various membrane holding potentials. We solve the system of equations numerically using the odeint integrator found within the SciPy library for the Python programming language, and the results for a particular set of parameter values and current stimulus is shown in Figure 4.

Figure 5 shows the change in the model's response to an array of current stimuli. As current stimulus is increased, one can see a transition from no action potential to a single action potential to a train of action potentials. Specifically, Figures 5(a) and 5(b) show a cell's response to $I_{ext} = 0.01nA$ and $I_{ext} = 0.02nA$ respectively. In both instances one sees that the stimulus injection is too weak to generate an action potential. Figure 5(c) shows the generation of a single action potential in response to $I_{ext} = 0.03nA$, whereas Figures 5(d) and 5(e) show how a train of action potentials is generated due to a stimulus of $I_{ext} = 0.04nA$ and $I_{ext} = 0.05nA$ respectively. Lastly, a case of over-stimulation can be seen in Figure 5(f), where $I_{ext} = 0.5nA$, and where too much stimulus caused the depression of this neuronal model. These dynamics reflect typical A-type neuron behavior, where one can observe either no action potential, a single action potential, or a train of action potentials, with an increase in frequency in response to an increase in stimulus intensity.

Model Parameters	Conductances for A-type neuron model
$[\text{Na}^+]_i = 8.9mM$	$\bar{g}_{\text{Na}_f} = 2.0500\mu S$
$[\text{Na}^+]_o = 154.0nM$	$\bar{g}_{\text{Na}_s} = 0.00001\mu S$
$[\text{K}^+]_i = 145.0mM$	$\bar{g}_{\text{Ca}_t} = 0.00035\mu S$
$[\text{K}^+]_o = 5.4mM$	$\bar{g}_{\text{Ca}_n} = 0.00100\mu S$
$[\text{Ca}^{2+}]_o = 2.0mM$	$\bar{g}_K = 0.00550\mu S$
$\tau_{\text{Ca}} = 4511.0ms$	$\bar{g}_A = 0.03500\mu S$
$E_{\text{Na}} = 72.7194mV$	$\bar{g}_D = 0.0100\mu S$
$E_K = -83.9282mV$	$\bar{g}_{K,\text{Ca}} = 0.00650\mu S$
$[B]_i = 0.001mM$	$\bar{g}_{B,\text{Ca}} = 0.000085\mu S$
$R = 8.314Jmole^{-1}K^{-1}$	$\bar{g}_{B,\text{Na}} = 0.000325\mu S$
$F = 96500Cmole^{-1}$	$\bar{I}_{\text{Ca}P} = 0.0243nA$
$T = 296K$	$\bar{I}_{\text{Na}K} = 0.275nA$
$K_{M,\text{Na}} = 5.46mM$	$c_m = 32.5pF$
$K_{M,\text{K}} = 0.621mM$	
$k_U = 100mM^{-1}mS^{-1}$	
$k_R = 0.238ms^{-1}$	
$Z_{\text{Ca}} = 2.0$	
$\gamma = 0.5$	
$r = 3$	
$n_b = 4$	
$Vol_i = 0.0127nl$	
$Vol_s = 0.0146nl$	

Table 6: A-type model parameters and conductances for each ionic channel [2] .

3.2 The Effect of Toxin

3.2.1 Tetrodotoxin

Tetrodotoxin (TTX) is a potent neurotoxin, first believed to be present exclusively in the pufferfish of family *Tetraodontidae*, from which it derives its name. It has long been a topic of debate whether TTX is produced by the pufferfish itself, or taken from the outside. This belief was abandoned in 1964 when TTX was detected in the Californian newt [8]. Since then, TTX has been detected in various marine and terrestrial species. It has been experimentally determined that pufferfish accumulate tetrodotoxin through the food chain, starting with marine bacteria. TTX is one of the most powerful neurotoxins, is highly toxic to humans, and to date, has no antidote [8].

TTX is a potent blocker of the fast Na^+ voltage-gated channel. It inhibits the firing of action potentials in neurons by binding to the voltage-gated sodium channels

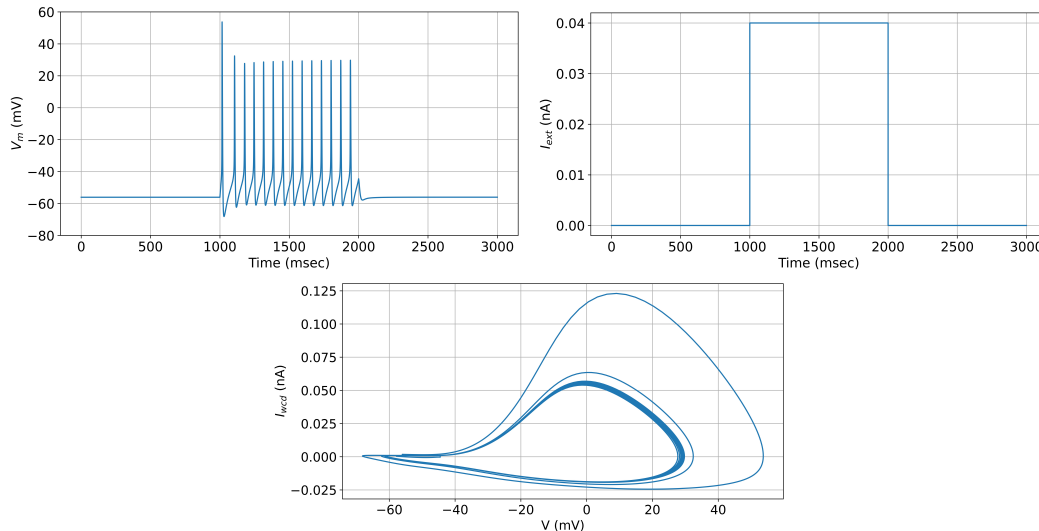


Figure 4: Voltage, V_m , response to a stimulus injection of 0.04 nA, with all parameters at default values. A train of action potentials can be observed (top left) due to a stimulus current (top right). A whole cell current density phase portrait (bottom), shows a closed path in the phase plane as the neuron progresses through the action potentials (top left).

in nerve cell membranes, thus blocking the passage of sodium ions (responsible for the rising phase of an action potential) into the neuron. This prevents the nervous system from carrying messages, and thus prevents muscles from contracting in response to nervous stimulation [9]. The severity of symptoms caused by TTX depends on the ingested dose. Symptoms typically include tingling of tongue and lips, headache, vomiting, muscle weakness, ataxia, and even death due to respiratory and/or heart failure [8].

Table 7 displays TTX's fast sodium channel blocking properties. When fast sodium conductance g_{Na_f} is at its default value of $2.05\mu S$, and stimulus is $0.04nA$, we see that action potential generation is normal and uninterrupted. However, when TTX is present in the system, it mimics the Na^+ , but because of its size, it cannot get in the channel, and fast sodium conductance goes to zero so that $g_{Na_f} = 0$, which in turn, abolishes the action potential generation. Given that TTX blocks the voltage-gated sodium channel and causes paralysis, its potential use as a pain reliever is being explored.

3.2.2 4-Aminopyridine

4-Aminopyridine (4-AP) is a simple, but impactful, organic chemical compound [10]. In 1963, 4-AP was developed and marketed as an avicide under the name Avitrol. It remains the most popular avicide registered at the US Environmental Protection Agency for the control of certain pest birds that destroy crops and grain. However, given its toxicity to non-target species, it has been banned in many cities in the US in recent years [10].

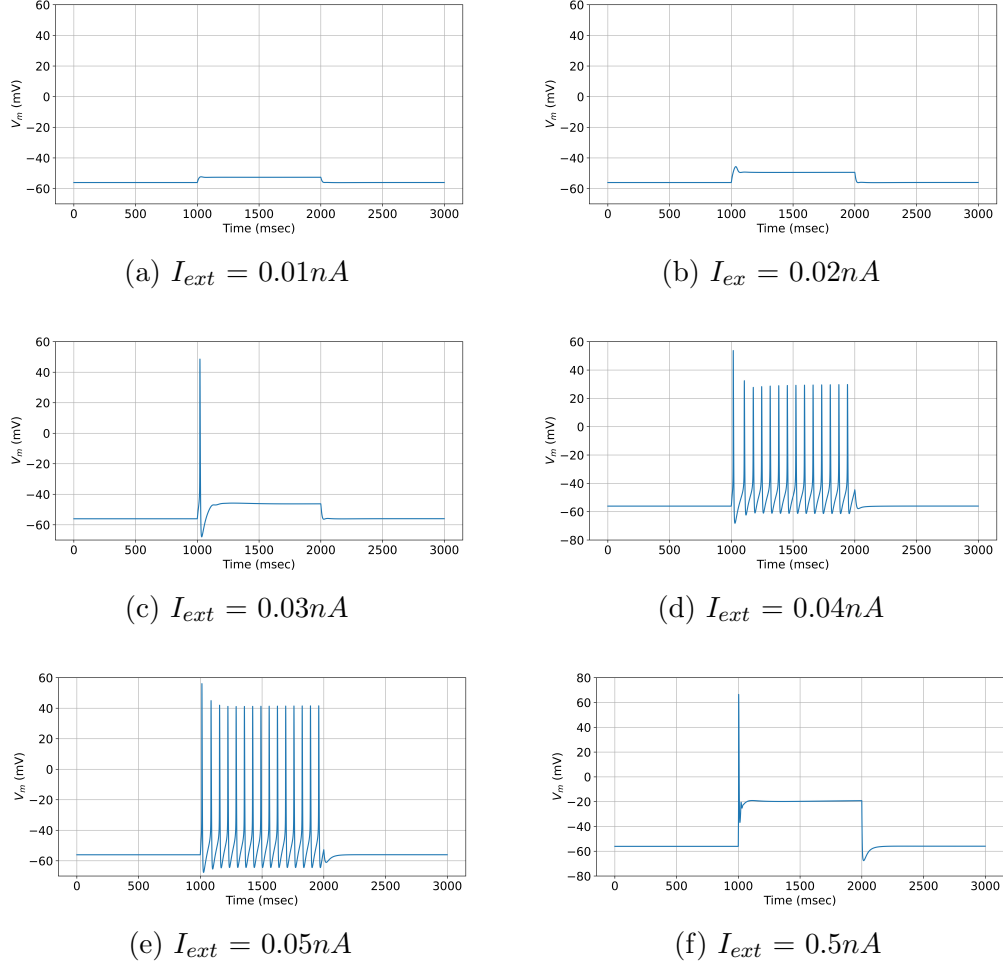


Figure 5: Voltage, V_m response to a current stimulus injection of (a) $0.01nA$, and (b) $0.02nA$. In both instances the stimulus injection is too weak to generate any action potentials. (c) Voltage, V_m response to a stimulus injection of $0.03nA$, which causes a single action potential. (d) Voltage, V_m response to a current stimulus injection of $0.04nA$, and (e) $0.05nA$. In both (d) and (e), a train of action potentials is observed, with the train in (e) showing a stronger intensity. Lastly, a case of overstimulation is shown in (f), due to a stimulus injection of $0.5nA$. Too much stimulus caused the depression of this neuron.

As an avicide, 4-AP is mixed into grain and set out as bait. It elicits toxicity to all grain-consuming birds. Moreover, any grain consuming organisms, such as livestock, are at risk from ingestion of the chemical compound. Human exposure is possible in industrial and manufacturing settings. While 4-AP is rapidly absorbed from the gastrointestinal tract, it can also be absorbed through the skin [10]. Reported toxicities among humans are of acute nature. At toxic doses, 4-AP blocks certain K^+ ion channels, which results in hyperactivity, convulsions, and seizures, as demonstrated in Table 8.

The compound has received a large amount of attention due to its excitatory

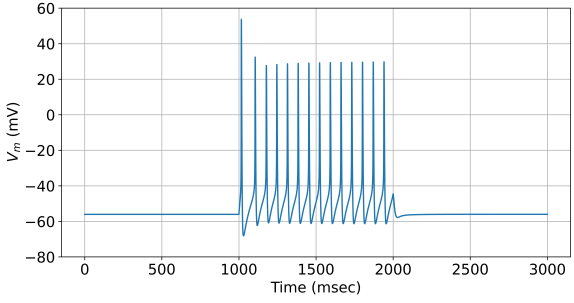
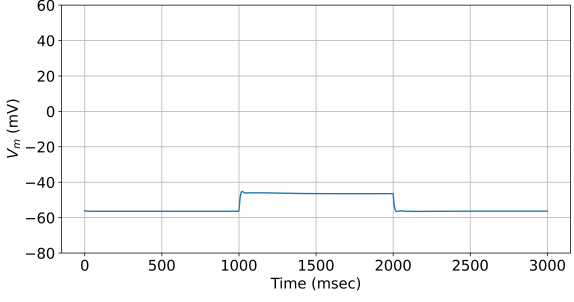
Stimuli Category	Figure
Pufferfish (<i>Tetraodontidae</i>)	 <p data-bbox="1235 520 1386 541">https://the-most-extreme.fandom.com/wiki/Pufferfish</p>
$g_{Na_f} = 2.05\mu S$	
$g_{Na_f} = 0.0\mu S$	

Table 7: Tetrodotoxin (TTX) is a powerful neurotoxin found in pufferfish (top right), from which it derives its name. When fast sodium conductance, g_{Na_f} , is at its default value of $2.05\mu S$, and a stimulus of $0.04nA$ is applied, a normal and uninterrupted train of action potentials is observed (middle). When TTX is present in the system, the sodium channel is blocked so that $g_{Na_f} = 0.0\mu S$, and the action potentials are no longer generated (bottom).

effects. Indeed, 4-AP may be useful as a pharmacological drug in neurological diseases such as Multiple Sclerosis (MS) and for spinal cord injury. The improvement of visual function and motor skills in patients with MS have been attributed to 4-AP [11]. Spinal cord injury patients have also seen improved sensory, motor, and pulmonary function, with a decrease in spasticity and pain. Recent clinical studies have shown that 4-AP is capable of reversing the effects of tetrodotoxin poisoning in animals, but its effectiveness as an antidote in humans has not yet been tested [12].

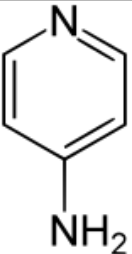
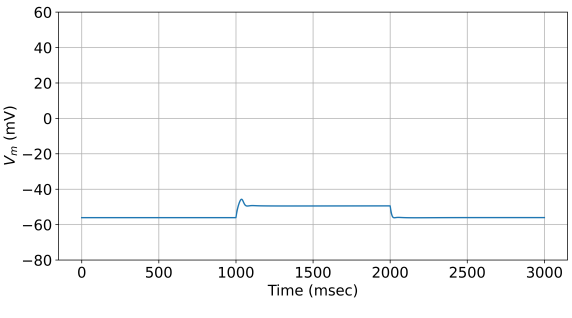
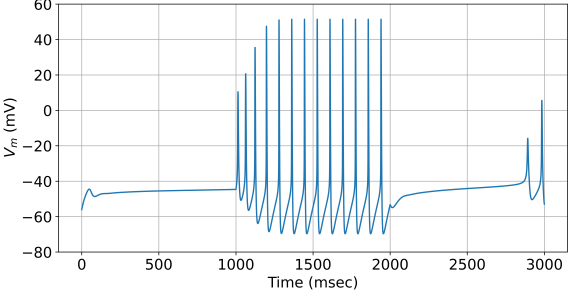
Stimuli Category	Figure
4-Aminopyridine	 https://en.wikipedia.org/wiki/4-Aminopyridine
$g_K = 0.0055\mu S$	
$g_K = 0.0\mu S$	

Table 8: 4-Aminopyridine (4-AP) is a simple organic chemical compound (top), and is toxic to humans. When potassium conductance is $g_K = 0.0055\mu S$ and a stimulus injection of $0.02nA$ is applied, no action potential is observed (middle). At toxic doses, 4-AP blocks potassium ion channels, and $g_K = 0.0\mu S$, which results in hyperactivity (bottom).

3.2.3 Iberitoxin

Iberitoxin (IbTX) is an ion channel toxin refined from the Indian Red Scorpion, and is able to block large-conductance calcium-activated potassium channels. It selectively inhibits the current by decreasing the probability of opening, as well as the length of open time of the channel [13]. The venom produces paralysis and cardiopulmonary reactions, such as myocarditis and circulatory derangement.

Table 9 shows the effects of IbTX. In its absence, $g_{K,Ca} = 0.0065\mu S$, and a healthy train of action potentials can be seen. However in the presence of IbTX so that $g_{K,Ca} = 0.0\mu S$, the number of action potentials is increased, and they become progressively depressed, i.e. the action potential amplitude decreases, which is indicative of the paralyzed muscles of a scorpion's prey.

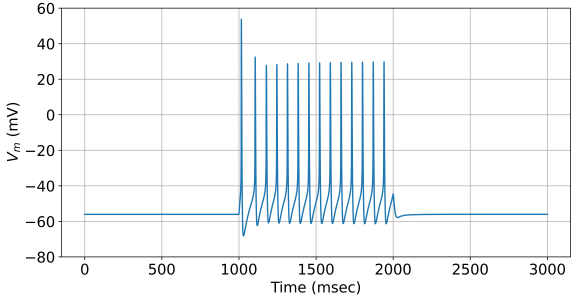
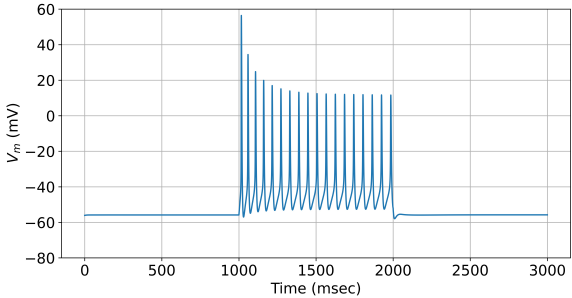
Stimuli Category	Figure
Indian Red Scorpion	 <p data-bbox="768 562 1187 583">https://en.wikipedia.org/wiki/Hottentottatamulus</p>
$g_{KCa} = 0.0065\mu S$	
$g_{KCa} = 0.0\mu S$	

Table 9: Iberitoxin (IbTX) is an ion channel toxin refined from the Indian Red Scorpion (top). IbTX blocks calcium-activated potassium channels. In the absence of IbTX, with $g_{KCa} = 0.0065\mu S$, and with a stimulus injection of $0.04nA$, a healthy, uninterrupted train of action potentials can be observed (middle). In the presence of IbTX, $g_{KCa} = 0.0\mu S$, the number of action potentials is increased, and they become progressively depressed (bottom).

4 Summary and Remarks

The work contained in this thesis starts with the groundbreaking work of Alan Hodgkin and Andrew Huxley. They determined how an electrical signal is generated and propagated along an axon. Their series of electrophysiological experiments on the giant axon of the squid led to the development of a mathematical model which consists of a set of differential equations that describe the ionic basis of the action potential. This became widely known as the Hodgkin-Huxley model, and it serves as a basis of most neuronal models today. The classical Hodgkin-Huxley model consists

of three types of ion currents, namely sodium, potassium, and leakage. The model, as well as its equivalent circuit, were considered in the first part of this thesis. The system of nonlinear differential equations was solved using an ODE solver in the Python programming language. Numerical results accurately described experimental results, including the duration and form of the action potential, the amplitude of the spike, oscillations, and ionic changes with respect to sodium and potassium.

The Hodgkin-Huxley model served as a template for an expanded version which models the dynamics of A-type nodose sensory neurons, and was used to study the effects of known ion channel blockers such as TTX, 4-AP, and IbTX. Similar to the Hodgkin-Huxley model, the extended model was solved numerically. In particular, we tested the model using an array of different current stimulus injections, and the results were found to accurately reflect a typical A-type neuron's behavior.

Moreover, various current stimulation intensities were considered in order to reproduce responses to different toxins. First, TTX, was considered, which is typically found in pufferfish, and is highly toxic to humans. TTX has sodium channel blocking properties, and when present it mimics the fast sodium ion channel, thus abolishing the action potential generation. Next, 4-AP the simple, yet impactful chemical compound was considered. It's mostly used as an avicide against grain-consuming birds, but it is acutely toxic to humans. When ingested in toxic doses, it blocks voltage-sensitive potassium channels, which can lead to seizures. Lastly, IbTX was considered, a toxin found in the Indian Red Scorpion. This toxin blocks the large-conductance calcium-activated potassium channels. In the presence of IbTX we see that the number of action potentials is increased, but their amplitude is progressively decreasing, which is indicative of the paralyzed muscles of their prey.

The development of this model, its ability to accurately simulate the electrical behavior of A-type nodose neurons, and its relative ease of use, offers an opportunity for exploration for those who may be lacking mathematical and computational background. Furthermore, it opens up a number of exciting further investigations, such as the study of C-type nodose neurons, and the inclusion of experimental data to parametrize the model for different experimental scenarios.

References

- [1] A. L. Hodgkin and A. F. Huxley, “A quantitative description of membrane current and its application to conduction and excitation in nerve,” The Journal of Physiology, vol. 117, no. 4, pp. 500–544, 1952.
- [2] J. H. Schild, J. W. Clark, M. Hay, D. Mendelowitz, M. C. Andersen, and D. Kunze, “A- and C- type rat nodose sensory neurons: Model interpretations of dynamic discharge characteristics,” Journal of Neurophysiology, vol. 71, no. 6, pp. 2338–2357, 1994.
- [3] Khanna Aarushi, “Action potential.” <https://teachmephysiology.com/nervous-system/synapses/action-potential/>, 2022. [Online; accessed April-2022].
- [4] H. F. Lodish, A. Berk, C. Kaiser, M. Krieger, P. M. Scott, A. Bretscher, H. L. Ploegh, and P. T. Matsudaira, Molecular Cell Biology. W.H. Freeman, 2008.
- [5] M. E. Nelson, Electrophysiological Models In: Databasing the Brain: From Data to Knowledge, pp. 285–301. Wiley, 2004.
- [6] M. Nelson and J. Rinzel, The Book of Genesis, ch. 4 The Hodgkin—Huxley Model. Springer, 1998.
- [7] G. Wulfram, M. W. Kistler, R. Naud, and L. Paninski, Neuronal Dynamics. Cambridge University Press, 2014.
- [8] J. Lago, L. P. Rodríguez, L. Blanco, J. M. Vieites, and A. G. Cabado, “Tetrodotoxin, an extremely potent marine neurotoxin: Distribution, toxicity, origin and therapeutical uses,” Marine Drugs, vol. 13, no. 10, 2015.
- [9] V. Bane, M. Lehane, M. Dikshit, A. O’Riordan, and A. Furey, “Tetrodotoxin: Chemistry, toxicity, source, distribution and detection,” Toxins, vol. 6, no. 2, 2014.
- [10] P. Wexler, Encyclopedia of Toxicology, pp. 194–195. Academic Press, 2014.
- [11] H. A. M. Van Diemen, C. H. Polman, J. C. Koetsier, A. C. Van Loenen, J. J. P. Nauta, and F. W. Bertelsmann, “4-aminopyridine in patients with multiple sclerosis,” Clinical Neuropharmacology, vol. 16, no. 3, 1993.
- [12] F. C. Chang, D. L. Spriggs, B. J. Benton, S. A. Keller, and B. R. Capacio, “4-aminopyridine reverses saxitoxin (stx)- and tetrodotoxin (ttx)-induced cardiorespiratory depression in chronically instrumented guinea pigs,” Fundamental and Applied Toxicology, vol. 38, no. 1, 1997.
- [13] S. Candia, M. L. Garcia, and R. Latorre, “Mode of action of iberiotoxin, a potent blocker of the large conductance Ca(2+)-activated K+ channel,” Biophysical Journal, vol. 63, no. 2, 1992.